Revision 4

Precipitation and dissolution of chromite by hydrothermal solutions in the Oman ophiolite: new behavior of Cr and chromite

Shoji Arai[1],* and Norikatsu Akizawa[1]

[1]Department of Earth Sciences, Kanazawa University, Kakuma, Kanazawa 920-1192, Japan.

*e-mail: ultrasa@staff.kanazawa-u.ac.jp

Abstract

Chromite is a typical refractory igneous mineral, precipitated from mafic magmas at relatively high temperatures. Chromites commonly occur in sedimentary, metamorphic and metasomatic rocks, where they are interpreted as relics of an igneous phase and serve as the source of Cr for low-temperature Cr-bearing minerals. We present evidence for the nucleation of chromite within hydrothermal solutions. We have found minute euhedal chromite grains enclosed by uvarovite (Ca-Cr garnet) in a diopsidite, metasomatically replacing the layered gabbro of the Oman ophiolite. The uvarovite shows oscillatory concentric zoning in terms of Cr# (= Cr/(Cr + Al)), and the chromite is embedded only in the high-Cr# zones of the uvarovite. Another diopsidite, replacing peridotite in the underlying upper mantle section,

contains xenocrystic chromite, which is partly dissolved. This suggests that a hydrothermal solution collected Cr by partial to total dissolution of chromite within the upper mantle and precipitated chromite, along with high-Cr# uvarovite, within the lower crust upsection. The metasomatic agent involved was a CO_2-, SO_2- and Cl-bearing hydrothermal solution containing appreciable silicate components that could carry Cr, possibly as a complex. The hydrothermal chromite is similar in chemistry to that commonly found in igneous rocks (e.g., Cr# = 0.8, $Mg/(Mg + Fe^{2+})$ = 0.1-0.2, TiO_2 <0.3 wt% and $Fe^{3+}/(Cr + Al + Fe^{3+})$, up to 0.3), but its Cr# is clearly different from that of mantle chromite (0.6-0.7) in peridotites and chromitites from the Oman ophiolite. The results from this study suggest that a hydrothermal origin is possible for chromites in ultramafic rocks that have experienced fluid activity assuming that there is sufficient chromite at the fluid source.

Keywords: hydrothermal chromite, uvarovite, diopsidite, Oman ophiolite

INTRODUCTION

Chromium is important in mafic and ultramafic rocks (Liang and Elthon 1989), in industry, and the environment (Motzer and Todd Engineers 2004), although its behavior in

nature is not fully understood. Chromite is a typical refractory magmatic mineral (Irvine 1965; Arai 1992) and the main reservoir for Cr in rocks. During alteration, Cr is extracted from chromite with difficulty but is easily liberated from Cr-bearing silicates (Oze et al. 2004). Cr^{3+} is mobile only over a limited distance during alteration or metamorphism of rocks (Treloar 1987; Martin 2009; Klein-BenDavid et al. 2011). Secondary Cr-rich minerals, such as uvarovite (Ca-Cr garnet), most frequently form at the expense of the primary chromite, which serves as their Cr source (Treloar 1987; Proenza et al. 1999; Taguchi et al. 2012).

In this study we describe partially dissolved chromite in a diopsidite from the Oman ophiolite (e.g., Lippard et al. 1986) that has metasomatically replaced mantle peridotite (Python et al. 2007). In the same locality new chromite has nucleated in another diopsidite replacing a lower crustal Cr-poor gabbro (Akizawa et al. 2011). The behavior of the hydrothermally deposited Cr and chromite is discussed and interpreted.

GEOLOGICAL BACKGROUND AND PETROGRAPHY

Diopsidites occur in the mantle section of the Oman ophiolite as a result of sub-oceanic hydrothermal activity (Python et al. 2007). They are possibly a reaction product between mantle rocks and hydrothermal fluids (> 800 ºC), rich in silicate components, circulating

52 downward from the seafloor through the crust into the upper mantle (Python et al. 2007). We
53 recognized two types of diopsidite from the Wadi Fizh, northern Oman ophiolite (Akizawa
54 and Arai 2009). One is from the crustal section (= crustal diopsidite), replacing a layered
55 gabbro (Fig. 1a-c). It is about 50 meters higher than the top of the Moho transiton zone
56 (MTZ) (Akizawa et al. 2011). Here the MTZ is mainly composed of dunite and wehrlite and
57 is remarkably thin, 10 to 15 m, in this particular area of the Oman ophiolite (Akizawa and
58 Arai 2009; Akizawa et al. 2012). The other diopsidite is located in the uppermost mantle
59 section (mantle diopsidite). It is about 20 meters below the top of the MTZ and replaces
60 mantle rock (Fig. 1d,e).
61 The crustal diopsidite is grayish on the outcrop with bright green-white
62 uvarovite-anorthite pockets that sometimes contain black chromite dots (Fig. 1b,c). Accessory
63 minerals include chlorite, titanite, pumpellyite, and epidote. The latter two minerals form
64 veinlets, indicating that they are of late stage origin. The mantle diopsidite forms a dike
65 within the dunite (locally harzburgite) and is whitish but locally greenish with numerous
66 chromite grains (Fig. 1d,e). It is comprised mainly of diopside (>90 volume %) with
67 subordinate grossular (Ca-Al garnet). The chromite grains sometimes form parallel thin (< 5
68 mm) seams in the mantle diopsidite (Fig. 1e).

In the crustal diopsidite, uvarovite, which is skeletal and full of inclusions of other minerals such as anorthite and chlorite (Fig. 2a,b), shows an oscillatory, concentric zonal texture with respect to the Cr# (= Cr/(Cr + Al)) (Fig. 2c). Euhedral chromite is enclosed as fine grains in the uvarovite (Fig. 1a, b), and is distinctly different in appearance from that in altered chromitites (e.g., Proenza et al. 1999). The fine chromite grains are contained solely in the high-Cr# zones of the oscillatory-zoned uvarovite (Fig. 2c). Coarse, discrete, chromite grains are also skeletal and show concentric, oscillatory zoning with respect to the Cr# (Fig. 2d, e). It is noticeable that a hydrothermal mineral such as chlorite apparently takes part in chromite oscillatory zoning. The chlorite plays a role similar to that of an "Al-rich spinel" in the zoning (Fig. 2d, e). This also means the almost simultaneous crystallization of a typical non-magmatic mineral such as chlorite with chromite.

Chromite grains in the greenish part of the mantle diopsidite (Fig. 1d) differ in texture. Some of them show irregular anhedral morphologies, suggesting dissolution to varying degrees (Fig 3a). A thin (~ 1 μm) chromite film commonly fills the grain boundaries of the diopside adjacent to the coarse anhedral chromite grains (Fig. 3a-c). Other grains from the chromite seams are nearly euhedral, although cracked, and contain globular silicate inclusions (Fig. 3d) similar to chromite in chromitite (e.g., Borisova et al. 2012). The inclusions are,

however, now replaced with grossular and chlorite (Fig. 3d), although they may have initially been comprised of pargasite, phlogopite, and pyroxenes (e.g., Borisova et al. 2012). The diopsidite here probably replaced mainly a dunite with local chromite concentrations (or thin chromite seams). These seams are visible where the diopside is greenish (Fig. 1d,e).

To identify phases in micro-fluid inclusions trapped mainly in diopside and anorthite from the crustal diopsidite, we used a micro-Raman system (HORIBA JOBIN YVON, LabRAM HR-800) equipped with a 532 nm Nd-YAG laser (Showa Optoronics Co.,Ltd, J100GS-16) and an optical microscope (Olympus, BX41) (see Arai et al., 2012). The fluid inclusions are less than 10 μm across, and show negative crystal forms with a bubble and with or without daughter minerals. Raman spectroscopic analysis indicated the fluid inclusions are comprised mainly of H_2O, though daughter minerals of calcite and anhydrite were identified in fluid inclusions from the anorthite. The shape of Raman spectra in the O-H stretching region (2800 to 3800 cm^{-1}) of the H_2O-rich fluid inclusions suggests 10 to 20 wt% of NaCl solution (Mernagh and Wilde, 1989; Frezzotti et al., 2012). This is consistent with our preliminary laser ICP-MS analysis; Na was detected on fluid inclusions in titanite weheas not detected on inclusion-free parts. No peaks for CO_2 , e.g. at 1388 cm-1 and 1285 cm-1, were detected on the Raman spectra of the fluid inclusions, indicationg the $CO_2/(H_2O + CO_2)$ ratio

is quite low, < 2~3 mole% (Azbej et al., 2007).

MINERAL CHEMISTRY

Minerals were analyzed using a JEOL wave-length dispersive electron probe X-ray microanalyzer (JXA8800R) at Kanazawa University. During conventional quantitative spot analysis, analytical conditions were 10-kV accelerating voltage and a 12-nA electron beam current with a 3-μm beam diameter. For the elemental distribution maps (Figs. 2c,e and 3c), a 20 kV accelerating voltage and a 100 nA probe current with a beam diameter of less than 1 μm were used. Natural and synthetic materials (quartz, esklaite, wollastonite, fayalite, jadeite, $KTiPO_5$, corundum, manganosite, periclase and bunsenite) were used as standards. Dwell time and step intervals were 50 milli-seconds and 3 μm for uvarovite (Fig. 2c), and 40 milli-seconds and 0.5 μm for chromite (Fig. 2f and 3c). The Fe^{2+} and Fe^{3+} contents in chromite were calculated assuming stoichiometry. In the silicate minerals all the Fe was assumed to be Fe^{2+} except in the garnet where Fe was assumed to be Fe^{3+}. Standard deviations (1σ) are less than 1.0 wt% for major elements (> 10 wt% oxides) on diopside, anorthite and grossular, and about 2.2 wt% for Cr_2O_3 and 1.1 wt% for Al_2O_3 on Cr-poor and Cr-rich uvarovites. They are relatively hign in chromite cores, 1.1 and 1.0 wt% for Al_2O_3, 4.2

and 1.8 wt% for Cr_2O_3, 5.2 and 1.9 wt% for FeO, and 0.38 and 1.2 wt% for MgO, in the crustal diopsdite and mantle diopsidite, respectively. They are much lower in chromites from mantle harzburgite and chromitite.

Chromite from the crustal diopsidite is distinct in chemistry from that in the mantle diopsidite (Fig. 4; Table 1). The Cr# is higher in the former (≈ 0.8) than in the latter (≈ 0.6) (Fig. 4). The former is strongly zoned in $Fe^{3+}/(Cr + Al + Fe^{3+})$, which increases up to 0.3 at the rim (Fig. 4). For the chromite from the mantle diopsidite (Fig. 3a, d) the core is similar in composition to the mantle diopsidite chromite, and the rim, to the core of the crustal diopsidite chromite (Fig. 4), which are both characterized by a low Mg# (=$Mg/(Mg + Fe^{2+})$, < 0.2 (Table 1). They are similar both in the Mg# and $Fe^{3+}/(Cr + Al + Fe^{3+})$ to secondary chromite associated with chlorite from a podiform chromitite altered at relatively high temperatures (> the serpentinization temperature) (Arai et al. 2006) (Fig. 4). They are far lower in Mg# than chromites from ordinary podiform chromitites but are in approximately the same range in terms of $Fe^{3+}/(Cr + Al + Fe^{3+})$ (Fig. 4).

The uvarovite in the crustal diopsidite is higher in the Cr# (0.5-0.8) than uvarovite overgrown on chromite (Cr#=0.3-0.6) in altered chromitite from Oman (Fig. 5). Grossular in the mantle diopsidite is Cr-bearing (Table 1; Fig. 5). All the garnets described here are

assumed to be relatively anhydrous due to the fact that the electron microprobe analysis totals tend to average around 100 % (Table 1). Diopside is generally Mg-rich in the diopsidites overall, but its Mg# is lower in the crustal diopsidite (0.84-0.97) than in the mantle diopsidite (0.95-1.0) (Table 1). Diopside from the mantle diopsidite varies in Cr_2O_3 content, from almost nil to more than 2 wt.%. Chlorite, associated with chromite in the crustal diopsidite (Fig. 2d,e), is Cr-bearing high-Mg# clinochlore (Hey 1954) (Table 1). The anorthite Ca/(Ca + Na) ratio is higher than 0.93 in the two diopsidites (Python et al. 2007; Akizawa et al. 2011).

DISCUSSION

Hydrothermal formation of chromite

It is highly unlikely that the diopsidites described here formed as a magmatic intrusion (Python et al. 2007). Such highly calcic silicate melts have never been described in ophiolites. In addition, the diopsidite shares some minerals with skarns (Meinert 1992; Jamtveit et al. 1993). An H_2O-rich nature for the agent responsible for the formation of the diopsidites is supported by the presence of H_2O-rich inclusions in the diopside and anorthite from the crustal diopsidite. Growth of chlorite, together with chromite (Fig. 2d), also supports the hydrous nature of the fluid.

The pressure of formation of these diopsidites is estimated to be around 0.2-0.3 GPa from their position in the ophiolite stratigraphy in the region of the MTZ where the thickness of the crustal section is presumed to have reached at least 6 km (Reuber 1988). The temperature of formation of the crustal diopsidite is lower than the thermal stability limit of the Mg-rich clinochlore, 700-800 ºC at 0.3 GPa (Fawcett and Yoder 1966; Staudigel and Schreyer 1977). In contrast, the assemblage of anorthite + diopside + chlorite indicates that the temperature should have been higher than 500-550 ºC at 0.3 GPa (Rice 1983; Cheng and Greenwood 1989). This suggests that the hydrous crustal diopsidite were formed at temperatures slightly lower than the mantle diopsidites, which are anhydrous (> 800 ºC; Python et al. 2007). This temperature range is lower than the temperature of formation for ordinary rodingites (= hydrothermally altered mafic rocks in serpentinite), which are synchronous with serpentinization, i.e., 200~350ºC (e.g., Li et al. 2004; Frost et al. 2008; Bach and Klein 2009). The anhydrous nature of these garnets (Table 1) gives insight into the high-temperature character of the hydrothermal solution involved compared with the lower temperatures (mostly 200-350 ºC) for hydrogrossular-bearing rodingites (e.g., Barringa and Fyfe 1983; Esteban et al. 2003; Frost et al. 2008). This is consistent with the lower stabilization temperature of hydrogarnet compared to its higher temperature anhydrous equivalent (cf.

171 Pistorius and Kennedy 1960; Hsu 1980).

172 The concentric, oscillatory chemical zoning of uvarovite (Fig. 2c) indicates its progressive
173 growth outwards recording a periodic change in the Cr# of the solution present during
174 formation of the crustal diopsidite. The similar zonation in some chromite grains (Fig. 2e)
175 also indicates in-situ synchronous growth with uvarovite (Fig. 2c) from the same solution.
176 The enclosure of chromite exclusively in the high-Cr# growth zone in the uvarovite grains
177 strongly implies that the chromite as well as the high-Cr# uvarovite grew only when high-Cr#
178 solution pulses were available (Fig. 2c). This implies that co-existing chromite was not the Cr
179 source for uvarovite, as is normally the case in thermally altered rocks, especially chromitites
180 (Proenza et al. 1999) (Fig. 2c).

181 The texture and mode of occurrence indicate that the chromite grains were dissolved to
182 varying degrees in the mantle diopsidite (Fig. 3). The thin film of chromite filling diopside
183 grain boundaries (Fig. 3b, c) indicates the precipitation of chromite from a local Cr-rich
184 solution interstitial to the diopside grains. A mantle-rock (xenocrystic) origin for the chromite
185 grains in the mantle diopsidite is also supported by the chemical similarity between their
186 cores and mantle chromites (Fig. 4). In addition, the rim of the chromite from the mantle
187 diopsidite is similar in chemistry to the core of chromite grains from the crustal diopsidite

188 (Fig. 4). This implies that the hydrothermal solution took Cr up from chromite in the upper
189 mantle rocks (Fig. 3) and precipitated new chromite (Fig. 2a-e) within the lower crustal
190 gabbro, which is poor in Cr (Cr_2O_3<0.1 wt.%). Hydrothermal solutions, transported down
191 through the oceanic crust into the uppermost mantle, were responsible for the formation of the
192 mantle diopsidite (Python et al. 2007). This fluid was rich in Ca and probably Si (Python et al.
193 2007) but poor in Cr, and highly reactive with mantle olivine and chromite, precipitating
194 diopside and grossular.
195 Assuming constant volume, the basic reaction responsible for the formation of the mantle
196 diopsidite is: Mg_2SiO_4 (olivine)+ ($0.72CaO + 0.44SiO_2$) (solution) = $0.72CaMgSi_2O_6$
197 (diopside) + 1.28MgO (solution). The solution supplied both Ca and Si, and subtracted Mg
198 from the dunite protolith. Grossular possibly formed via the reaction: $MgAl_2O_4$ (spinel
199 component in chromite) + ($3CaO + 3SiO_2$) (solution) = $Ca_3Al_2Si_3O_{12}$ (grossular) + MgO
200 (solution). Precursor chromite was converted in part to a component in the diopside and in
201 part dissolved via the reaction: $FeCr_2O_4$ (chromite)+ ($CaO + SiO_2 + 0.5Al_2O_3$) (solution) =
202 $CaCrAlSiO_6$ (Cr-Ca Tchermak's component in diopside) + ($FeO + 0.5Cr_2O_3$) (solution).
203 The resultant Cr-bearing solution migrated upwards into the lower crust to
204 metasomatically convert the gabbro (mainly plagioclase + augite) into an anorthite diopsidite

coupled with the precipitation of chromite and uvarovite (Rai et al. 1989). The formation of uvarovite and anorthite in the crustal diopsidite, instead of grossular and diopside in the mantle diopsidite, may be due to the higher silica content in the gabbro-solution system in the crust than in the dunite-solution system in the MTZ because of the mass-balance reaction: $2CaCrAlSiO_6$ (Cr-Ca Tchermak's component in diopside) + $Ca_3Al_2Si_3O_{12}$ (grossular) + $2SiO_2$ = $Ca_3Cr_2Si_3O_{12}$ (uvarovite) + $2CaAl_2Si_2O_8$ (anorthite).

Chromium and Fe possibly formed a carbonate-sulfate-chloride complex in the solution, as evidenced by the presence of calcite and anhydrite daughter crystals as well as a NaCl solute in the fluid inclusions. Solubility of Cr in H_2O-CO_2-rich solutions, in the form of carbonate-complexes, is also suggested by experiments (Rai et al. 2007). Chlorite has been long known to play an important role in Cr dissolution in aqueous solution (e.g., Hall and Eyring, 1950; Gates and King, 1958). Dissolution of Cr, together with Fe, facilitates the precipitation of chromite from solution. Chromium was possibly hexavalent in the solution and subsequently reduced to be trivalent during chromite formation, although there is no evidence for the initial presence of Cr^{6+}. Reduction of Cr^{6+} to Cr^{3+} would have been facilitated if coupled with the oxidation of Fe^{2+} to Fe^{3+} (Motzer and Todd Engineers 2004). In reduced aqueous solutions Cr^{2+} could have also been mobile (cf. Borisova et al. 2012). However it is

unlikely that diopsidite formation occurred under reduced conditions since metal alloys are totally absent. This is in accordance with the higher temperature conditions here compared to the temperatures under which serpentinization (or rodingitization) could have occurred. These conditions could have resulted in a highly reducing fluid (e.g., Sleep et al. 2004)

Implications concerning mobility of Cr in lower crustal-upper mantle hydrothermal systems

The mobility of Cr in hydrothermal systems is probably more complicated than has been previously described. Solution and transportation of Cr via hydrothermal solutions can redistribute Cr within the oceanic mantle-crust system in the region of the hydrothermal activity near mid-oceanic ridge systems (Kelley et al. 2001). Chromium, initially distributed preferentially in chromite and pyroxenes in the upper mantle, is taken up, probably together with Fe, by circulating hydrothermal solutions and incorporated in metasomatised lower crustal rocks that contain Cr-rich minerals such as uvarovite and chromite. This process suggests another origin for chromite in metamorphic and metasomatized rocks. Euhedral chromites found in metasomatic or metamorphic rocks have been previously interpreted as relics, with or without chemical modification (e.g., Taguchi et al. 2012). However, the results

239 from this study indicate that chromites could also be precipitates from a hydrothermal
240 solution rich in carbonate, sulfate and chloride components. This also implies that Cr could be
241 mobile within the mantle wedge via the action of hydrous fluids released from the slab.
242 Olivine in strongly metasomatized peridotite xenoliths from Avacha volcano, Kamchatka,
243 which are representative of a mantle-wedge material beneath a volcanic front, contains
244 numerous fine grains of chromite (Ishimaru and Arai 2008). In accordance with the results
245 from this study, this suggests that these chromite grains could possibly have precipitated from
246 fluids active in that part of the mantle wedge during metasomatic alteration of the olivine
247 (Ishimaru and Arai 2011).
248 If conditions permit, even a chromitite (chromite ore) could possibly form as a result of
249 hydrothermal processes. The concentration of chromite as a result of fluid-aided processes
250 was an early idea regarding the formation of chromitites (e.g., Ross 1931), which are
251 selectively altered even when the peridotites are intact. Originally a hydrothermal origin for
252 chromitites was discounted by Arai (1978). This is because hydration can influence the
253 concentration of Al and Cr in chromitites, since chlorite is formed at the expense of the
254 Al-spinel component in chromite at higher temperatures than serpentine upon retrogressive
255 cooling (Arai 1978). The idea of a hydrothermal origin for chromitite can now be revived.

These include chromitites in which the chromite has a low Mg# and Fe^{3+} content, which previously were described as high-temperature altered chromitites (e.g., Arai et al. 2006), and not as an alteration product from igneous chromitites.

ACKNOWLEDGEMENTS

We thank J. Uesugi, A. Tamura, M. Python and S. Ishimaru for collaboration in the filed. We are grateful to T. Morishita and S. Ishimaru for their assistance in microprobe analysis. T. Mizukami and M. Miura guided us to perform Raman spectroscopic analysis. Critical comments by A.Y. Borisova, an anonymous referee, and D. Harlov were highly helpful in revision of the previous manuscript.

REFERENCES CITED

Akizawa, N. and Arai, S. (2009) Petrologic profile of peridotite layers under a possible Moho in the northern Oman ophiolite: an example from Wadi Fizh. Journal of Mineralogical and Petrological Sciences, 104, 389-394.

Akizawa, N., Arai, S., Tamura, A., Uesugi, J. and Python, M. (2011) Crustal diopsidites from the northern Oman ophiolite: evidence for hydrothermal circulation through suboceanic

Moho. Journal of Mineralogical and Petrological Sciences, 106, 261-266.

Akizawa, N., Arai, S. and Tamura, A. (2012) Behavior of MORB magmas at uppermost mantle beneath a fast-spreading axis: an example from Wadi Fizh of the northern Oman ophiolite. Contributions to Mineralogy and Petrology, 164, 601-625.

Arai, S. (1992) Chemistry of chromian spinel in volcanic rocks as a potential guide to magma chemistry. Mineralogical Magazine, 56, 173-184.

Arai, S. (1997) Control of wall-rock composition on the formation of podiform chromitites as a result of magma/peridotite interaction. Resource Geology, 47, 177-187.

Arai, S. (1978) Formation of chlorite corona around chromian spinel in peridotite and its significance. Geoscience Reports of Shizuoka University, 3, 9-15 (in Japanese with English abstract).

Arai, S., Ishimaru, S. and Mizukami, T. (2012) Methane and propane micro-inclusions in olivine in titanoclinohumite-bearing dunites from the Sanbagawa high-P metamorphic belt, Japan: hydrocarbon activity in a subduction zone and Ti mobility. Earth and Planetary Science Letters, 353-354, 1-11.

Azbej, T., Severs, M.J., Rusk, B.G. and Bodnar, R.J. (2007) In situ quantitiative analysis of individual H2O-CO2 fluid inclusions by laser Raman spectroscipy. Chemical Geology,

237, 255-263.

Bach, W. and Klein, F. (2009) The petrology of seafloor rodingites: Insights from geochemical reaction path modeling. Lithos, 112, 103-117.

Barringa, F. and Fyfe, W.S. (1983) Development of rodingite in basaltic rocks in serpentinites, East Liguria, Italy. Conbributions to Mineralogy and Petrology, 84, 146-151.

Borisova, A., Ceuleneer, G., Kamenetsky, V.S., Arai, S., Béjina, F., Abily, B., Bindeman, I.N., Polvé, M., de Parseval, P., Aigouy, T. and Pokrovski, G.S. (2012) A new view on the petrogenesis of the Oman ophiolite chromitites from microanalyses of chromite-hosted inclusions. Journal of Petrology, 53, 2411-2440.

Cheng, W. and Greenwood, H.J. (1989) The stability of the assemblage zoisite + diopside. Canadian Mineralogist, 27, 657-662.

Esteban, J.J., Cuevas, J., Tubía, M. and Yuska, I. (2003) Xenotolite in rodingite assmeblages from the Ronda peridotites, Betic Cordilleras, southern Spain. Canadian Mineralogist, 41, 161-170.

Frezzotti, M.L., Tecce, F. and Casagli, A. (2012) Raman spectroscopy for fluid inclusions analysis. Joural of Geochemical Exploration, 112, 1-20.

Frost, B.R., Beard, J.S., McCraig, A. and Condliffe, E. (2008) The formation of

micro-rodingites from IODP Hole U1309D: Key to understanding the process of serpentinization. Journal of Petrology, 49, 1579-1588.

Gates, H.S. and King, E.L. (1958) A study of the equilibria in acidic chromium (III) chloride solutions. Journal of the American Chemical Society, 80, 5011-5015.

Hall, H.T. and Eyring, H. (1950) The constitution of chromic salts in aqueous solution. Journal of the Americam Chemical Society, 72, 782-790.

Hey, M.H. (1954) A new review of chlorites. Mineralogical Magazine, 30, 277-292.

Hsu, L.C. (1980) Hydration and phase relations of grossular-spessartine garnets at P_{H2O} = 2 kb. Conbributions to Mineralogy and Petrology, 71, 407-425.

Irvine, T.N. (1965) Chromian spinel as a petrogenetic indicator. Part 1. Theory. Canadian Journal of Earth Sciences, 2, 648-672.

Ishimaru, S. and Arai, S. (2008) Nickel enrichment in mantle olivine beneath a volcanic front. Contributions to Mineralogy and Petrology, 156, 119-131.

Ishimaru, S. and Arai, S. (2011) Peculiar Ca-Mg-Si metasomatism along a shear zone within the mantle wedge: inference from fine-grained xenoliths from Avacha volcano, Kamchatka. Contributions to Mineralogy and Petrology, 161, 703-720.

Jamtveit, B., Wogelius, R.A. and Fraser, D.G. (1993) Zonation patterns of skarn garnets:

Records of hydrothermal system evolution. Geology, 21, 113-116.

Kelley, D.S., Karson, J.A., Blackman, D.K., Früh-Green, G.L., Butterfield, D.A., Lilley, M.D., Olson, E.J., Schrenk, M.O., Roe, K.K., Lebon, G.T., Rivizzigno, P. and the AT3-60 Shipboard Party (2001) An off-axis hydrothermal vent field near the Mid-Atlantic Ridge at 30º N. Nature, 412, 145-149.

Klein-BenDavid, O., Pettke, T. and Kessel, R. (2011) Chromium mobility in hydrous fluids at upper mantle conditions. Lithos, 125, 122-130.

Li, X.-P., Rahm, M. and Bucher, K. (2004) Metamorphic processes in rodingites of the Zermatt-Saas ophiolites. International Geology Review, 47, 28-51.

Liang, Y. and Elthon, D. (1989) Evidence from chromium abundances in mantle rocks for extraction of picrite and komatiite melts. Nature, 343, 551-553.

Lippard, S.J., Shelton, A.W. and Gass, I.G. (1986) The ophiolite of northern Oman, Geological Society Memoir 11, 178 p. Blackwell Scientific Publications, Oxford.

Martin, A.J. (2009) Sub-millimeter heterogeneity of yttrium and chromium during growth of semi-pelitic garnet. Journal of Petrology, 50, 1713-1727.

Meinert, L.D. (1992) Skarns and skarn deposits: Geoscience Canada, 19, 145-162.

Mernagh, T.P. and Wilde, A.R. (1989) The use of the laser Raman microprobe for the

341 determination of salinity in fluid inclusions. Geochimica et Cosmochimica Acta, 53,
342 765-771.
343 Motzer, W.E. and Todd Engineers (2004) Chemistry, geochemistry, and geology of
344 chromium and chromium compounds. In F. Guertin, C.P. Avakian and J.A. Jacobs, Eds.,
345 Chromium(VI) Handbook, p. 23-88. CRC Press, Boca Raton, Florida.
346 Normand, C. and Williams-Jones, A.E. (2007) Physicochemical conditions and timing of
347 rodingite formation: evidence from rodingite-hosted fluid inclusions in the JM Asbestos
348 mine, Asbestos, Quebec. Geochemical Transactions 2007, 8:11
349 doi:10.1186/1467-4866-8-11.
350 Oze, C., Fendorf, S., Bird, D.K. and Coleman, R.G. (2004) Chromium geochemistry in
351 serpentinized ultramafic rocks and serpentine soils from the Franciscan Complex of
352 California. American Journal of Science, 304, 67-101.
353 Pistorius, C.W.F.T. and Kennedy, G.C. (1960) Stability relations of grossularite at high
354 temperatures and pressures. American Journal of Science, 258, 247-257.
355 Pomonis, P., Tsikouras, B., Karipi, S. and Natzipanagiotou, K. (2008) Rodingite formation in
356 ultramafic rocks from the Koziakas ophiolite, western Thessaly, Greece: conditions of
357 matasomatic alteration, geochemical exchanges and T-$X(CO_2)$ evolutionary path. Canadian

Mineralogist, 46, 569-581.

Proenza, J., Solé, J. and Melgarejo, J.C. (1999) Uvarovite in podiform chromitite: The Moa-Baracoa ophiolitic massif, Cuba. Canadian Mineralogist, 37, 679-690.

Python, M., Ceuleneer, G., Ishida, Y., Barrat, J.-A. and Arai, S. (2007) Oman diopsidites: a new lithology diagnostic of very high temperature hydrothermal circulation in mantle peridotite below oceanic spreading centres. Earth and Planetary Science Letters, 255, 289-305.

Rai, D., Early, L.E. and Zachara, J.M. (1989) Environmental chemistry of chromium. Science of the Total Environment, 86, 15-23.

Rai, D., Moore, D.A, Jess, N.J., Rosso, K.M., Rao, L. and Heald, S.M. (2007) Chromium (III) hydroxide solubility in the aqueous K^+-H^+-CO_2-HCO_3^{2-} -H_2O system: a thermodynamic model. Journal of Solution Chemistry, 36, 1261-1285.

Reuber, I (1988) Complexity of the crustal sequence in the northern Oman ophiolite (Fizh and southern Aswad blocks): The effect of early slicing? Tectonophysics, 151, 137-165.

Rice, J.M. (1983) Metamorphism of rodingites: Part 1. Phase relations in a portion of the system CaO-MgO-Al_2O_3-SiO_2-CO_2-H_2O. American Journal of Science, 283-A, 121-150.

Ross, C.S. (1931) The origin of chromite. Economic Geology, 26, 540-545.

375 Sleep, N.H., Meibom, S., Fridriksson, Th., Coleman, R.G. and Bird, D.K. (2004) H_2-rich
376 fluids from serpentinization: geochemical and biotic implication. Proceedings of National
377 Academy of Sciences of the United States of America, 101, 12818-12823.
378 Taguchi, T., Satish-Kumar, M., Hokada, T. and Jayananda, M. (2012) Petrogenesis of Cr-rich
379 calc-silicate rocks from the Bandihalli supracrustal belt, Archean Dharwar Craton, India.
380 Canadian Mineralogist, 50, 705-718.
381 Treloar, P.J. (1987) The Cr-minerals of Outokumpu- Their chemistry and significance.
382 Journal of Petrology, 28, 867-886.
383
384 **Figure captions**
385
386 **Figure 1.** Diopsidites of hydrothermal origin from Wadi Fizh, Oman ophiolite. (**a**)
387 Chromite-bearing crustal diopsidite replacing layered gabbro (G) on the outcrop.
388 Uvarovite-rich part is greenish. (**b**) Hand specimen of the chromite-bearing uvarovite,
389 replacing gabbro (G). Grayish part around the gabbro (G) is rich in diopside, and the greenish
390 part contains uvarovite, anorthite, and chromite. (**c**) Hand specimen of diopsidite rich in
391 chromite (black dots). Grayish to whitish part is rich in diopside. (**d**) Hand specimen of the
392 crustal diopsidite. Black dots are chromite of mantle-rock (xenocrystal) origin. White to gray

part consists of Cr-poor diopside, and the greenish part around chromite is not uvarovite but Cr-rich diopside. (**e**) Mantle diopsidite replacing a dunitic rock in the Fizh MTZ. Note a seam of chromite (Chr) with greenish Cr-bearing diopside, which may be a remnant of chromite concentrations in the dunite host.

Figure 2. Uvarovite and chromite in the crustal diopsidite. (**a**) Photomicrograph (plane-polarized light) of an euhedral uvarovite grain (light green) full of inclusions. Black dots are chromite inclusions. (**b**) Close-up of one of the euhedral chromite inclusions in uvarovite (**a**). (**c**) Cr distribution map showing a concentric, oscillatory Cr distribution in the uvarovite grain (**a**). Note that chromite grains (white spots) are contained only in the high-Cr# (reddish) portions. White to warm colors show higher concentrations of Cr. (**d**) Back-scattered electron image of a relatively coarse skeletal chromite grain (white). Uvt, uvarovite. Chl, chlorite. An, anorthite. (**e**) Chromium distribution map showing the concentric, oscillatory distribution of Cr in the chromite grain (**d**). White to warm colors show higher concentrations of Cr. Note that chlorite is associated with the concentric zoning.

Figure 3. Chromite in the mantle diopsidite. (**a**) Photomicrograph (plane-polarized light)

of an anhedral chromite grain, possibly suggesting partial dissolution (black; Chr). Note the very thin chromite film (brown) along the diopside grain boundary (Di). (**b**) Close-up (plane-polarized light) of a part of the panel (**a**), showing the thin film of chromite (brown) along the diopside grain boundary. (**c**) Chromium distribution map of the area in (**a**) showing the chromite distribution. White to warm colors show higher concentrations of Cr. (**d**) Photomicrograph (reflected light) of a semi-euhedral chromite grain (Chr) in diopside (Di). Cracks and globular inclusions are filled by grossular (Grs) and chlorite (Chl). The chromite grain is interpreted to be intact or slightly modified. It represents a chromite relic from a mantle rock now metasomatically altered to diopsidite.

Figure 4. Chemical characteristics of chromites in diopsidites from Wadi Fizh, Oman ophiolite. Chromite compositional ranges are shown for MTZ peridotites (Akizawa and Arai 2009; Akizawa et al. 2012), high-temperature altered chromites in chromitites (Arai et al. 2006), and for ordinary podiform chromitites (Barnes and Roeder 2001). (**a**) Plot of Mg# vs. Cr#. Averaged chemical zonation trend from the core to the rim in the mantle diopsidite is shown by the arrow. (**b**) Ternary plot of Cr^{3+}, Fe^{3+}, and Al^{3+}. Averaged chemical zonation trends from the core to the rim are shown by arrows. In the crustal diopsidite chromite, the

427 rim is higher in Fe^{3+} than the core (broken line). The core is similar in chemistry to mantle

428 chromites, and the rim to the core of crustal diopsidite chromite (solid line).

429

430 **Figure 5.** Ternary plot of Cr^{3+}, Fe^{3+}, and Al^{3+} for garnets in diposidites from Wadi Fizh,

431 Oman ophiolite. The uvarovite associated with chromite in the crustal diopside is different in

432 chemistry from that in mantle chromitites from Wadi Hilti, northern Oman ophiolite. Garnet

433 from the mantle diopsidite, where chromite is of mantle-rock (xenocrystal) origin and

434 partially digested, is Cr-bearing grossular, not uvarovite.

This is a preprint, the final version is subject to change, of the American Mineralogist (MSA)
Cite as Authors (Year) Title. American Mineralogist, in press.
(DOI will not work until issue is live.) DOI: http://dx.doi.org/10.2138/am.2014.4473

Table 1 Chemical composition of main minerals

Rock type	Crustal diopsidite							Mantle diopsidite						Chromitite	Harzburgite
Mineral	Chromite		Uvarovite		Chlorite	Pl	Cpx	Chromite		Grossular		Cpx		Chromite	Chromite
Position	core	rim	Cr-rich	Cr-poor		core	core	core	rim	core	chr. rim	Cr-rich	Cr-poor	core	core
SiO_2	0.90	0.10	37.51	37.86	31.53	44.73	55.41	0.01	0.24	38.90	39.57	52.31	54.59	-	0.02
TiO_2	0.08	0.30	0.72	1.71	0.02	-	0.02	0.37	0.03	0.07	0.15	0.07	0.01	0.12	0.12
Al_2O_3	7.38	4.44	3.96	7.72	20.35	35.60	0.84	18.59	9.04	20.71	20.13	3.30	2.49	20.58	24.11
Cr_2O_3	54.90	39.05	22.02	12.30	1.46	0.04	-	42.88	55.70	2.22	3.07	2.39	0.04	49.30	40.03
Fe_2O_3	4.57	22.30	1.96*	5.34*		-	-	6.47	2.62	0.42*	0.68*	-	-	3.04	5.46
FeO	28.48	29.94	-	-	4.52*	0.05*	2.96*	24.50	27.84	-	-	0.81*	1.05*	11.54	18.79
MnO	0.54	1.55	0.10	0.04	0.05	-	0.00	0.63	1.14	-	0.04	0.03	0.01	0.24	0.35
MgO	2.71	1.06	0.50	0.19	30.18	-	16.58	6.88	3.41	0.03	0.37	16.34	16.97	15.59	11.08
CaO	0.31	0.10	33.65	34.92	0.12	19.65	25.65	-	0.43	38.73	36.60	26.17	25.89	0.01	-
Na_2O	0.11	-	0.00	0.00	-	0.39	0.12	0.00	-	-	0.00	0.21	0.33	0.01	-
K_2O	0.00	0.00	0.00	0.00	-	0.01	-	0.00	-	-	-	0.00	0.01	-	-
NiO	0.00	0.16	0.01	0.01	0.13	-	0.05	0.18	-	0.01	-	0.02	0.07	0.14	0.07
Total	99.97	99.01	100.43	100.09	88.35	100.46	101.62	100.51	100.46	101.09	100.62	101.66	101.45	100.57	100.04
O	4	4	12	12	28	8	6	4	4	12	12	6	6	4	4
Si	0.032	0.004	3.035	3.024	5.893	2.058	1.989	0.000	0.008	2.933	2.984	1.883	1.951	-	0.001
Ti	0.002	0.008	0.044	0.103	0.003	-	0.000	0.009	0.001	0.004	0.008	0.002	0.000	0.003	0.003
Al	0.305	0.194	0.378	0.726	4.482	1.930	0.035	0.713	0.370	1.840	1.788	0.140	0.105	0.737	0.881
Cr	1.523	1.142	1.408	0.776	0.216	0.001	-	1.102	1.528	0.132	0.183	0.068	0.001	1.184	0.981
Fe^{3+}	0.121	0.621	0.119	0.321	-	-	-	0.158	0.068	0.024	0.039	-	-	0.070	0.127
Fe^{2+}	0.836	0.926	-	-	0.707	0.002	0.089	0.666	0.808	-	-	0.024	0.031	0.293	0.487
Mn	0.016	0.048	0.007	0.0025	0.007	-	0.000	0.017	0.034	0.000	0.002	0.001	0.000	0.006	0.009
Mg	0.142	0.058	0.060	0.022	8.405	-	0.887	0.333	0.176	0.003	0.042	0.876	0.903	0.706	0.512
Ca	0.012	0.004	2.916	2.987	0.023	0.968	0.986	-	0.016	3.128	2.956	1.009	0.991	0.000	-
Na	0.007	-	0.000	0.000	-	0.034	0.008	0.000	-	0.000	0.000	0.015	0.023	0.000	-
K	0.000	0.000	0.000	0.000	-	0.000	-	0.000	-	0.000	-	0.000	0.000	-	-
Ni	0.000	0.005	0.001	0.001	0.019	-	0.001	0.005	-	0.001	-	0.001	0.002	0.004	0.002
Total	2.996	3.010	7.968	7.962	19.755	4.994	3.997	3.005	3.008	8.065	8.003	4.019	4.008	3.003	3.002
Mg#	0.145	0.129			0.922		0.909	0.3335	0.1791			0.9729	0.9665	0.707	0.512
Cr#	0.833	0.812	0.7885	0.517	0.046			0.6074	0.8052	0.097	0.132			0.616	0.527
An						96.6									

* All Fe is assumed to be Fe^{2+} or Fe^{3+}. An, anorthite. Di, diopside.

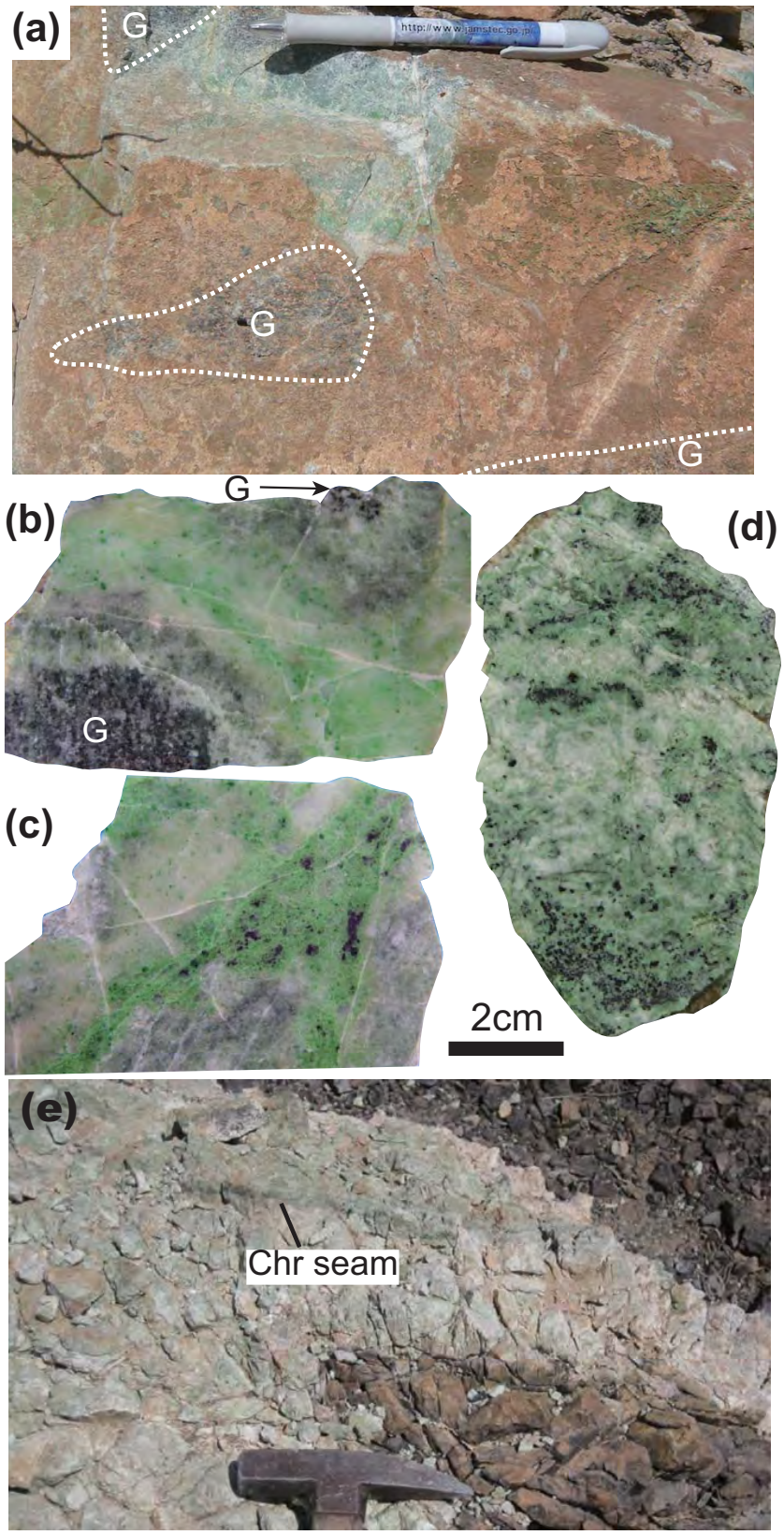

Figure 1 Arai & Akizawa

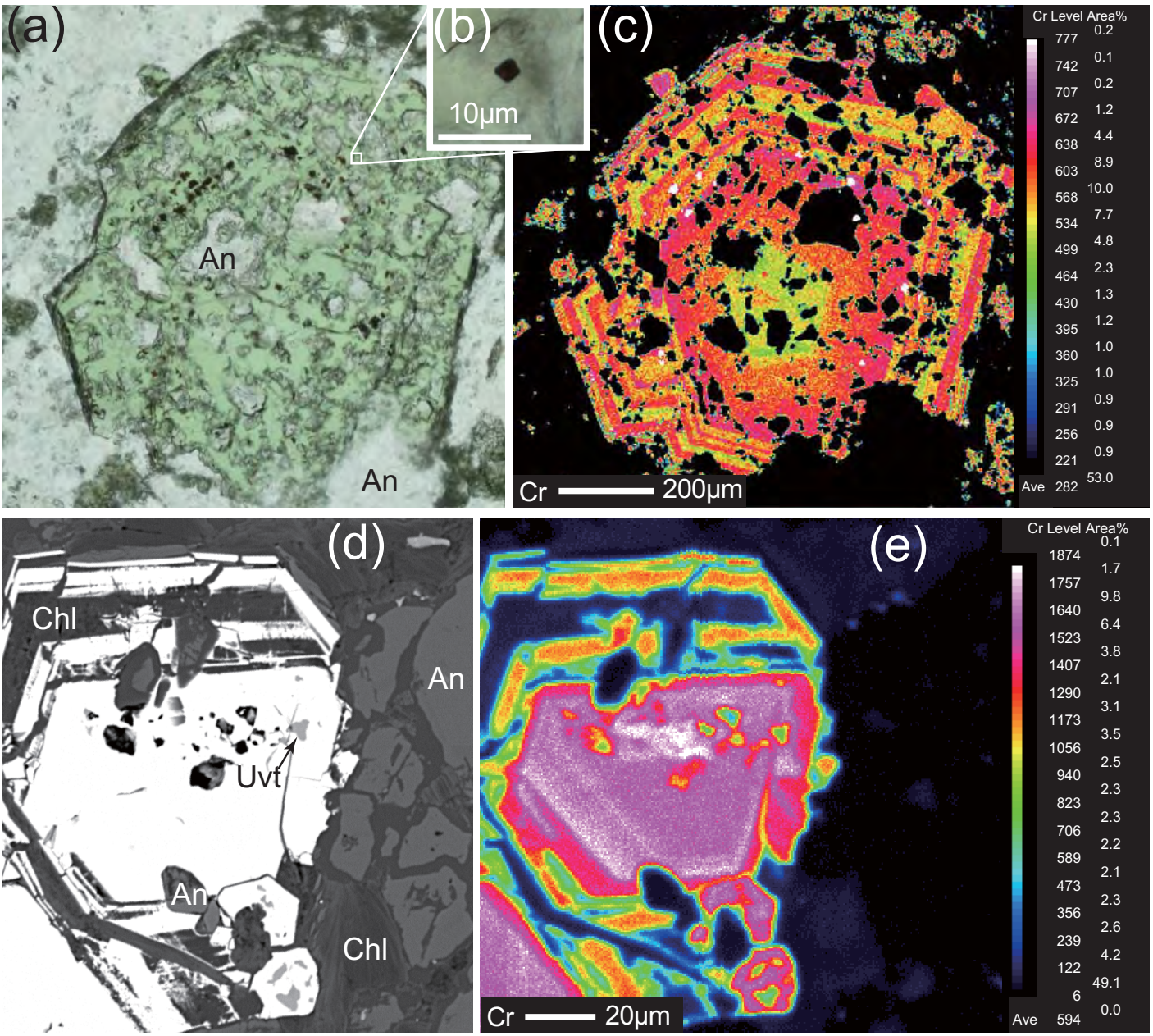

Figure 2 Arai & Akizawa

This is a preprint, the final version is subject to change, of the American Mineralogist (MSA)
Cite as Authors (Year) Title. American Mineralogist, in press.
(DOI will not work until issue is live.) DOI: http://dx.doi.org/10.2138/am.2014.4473

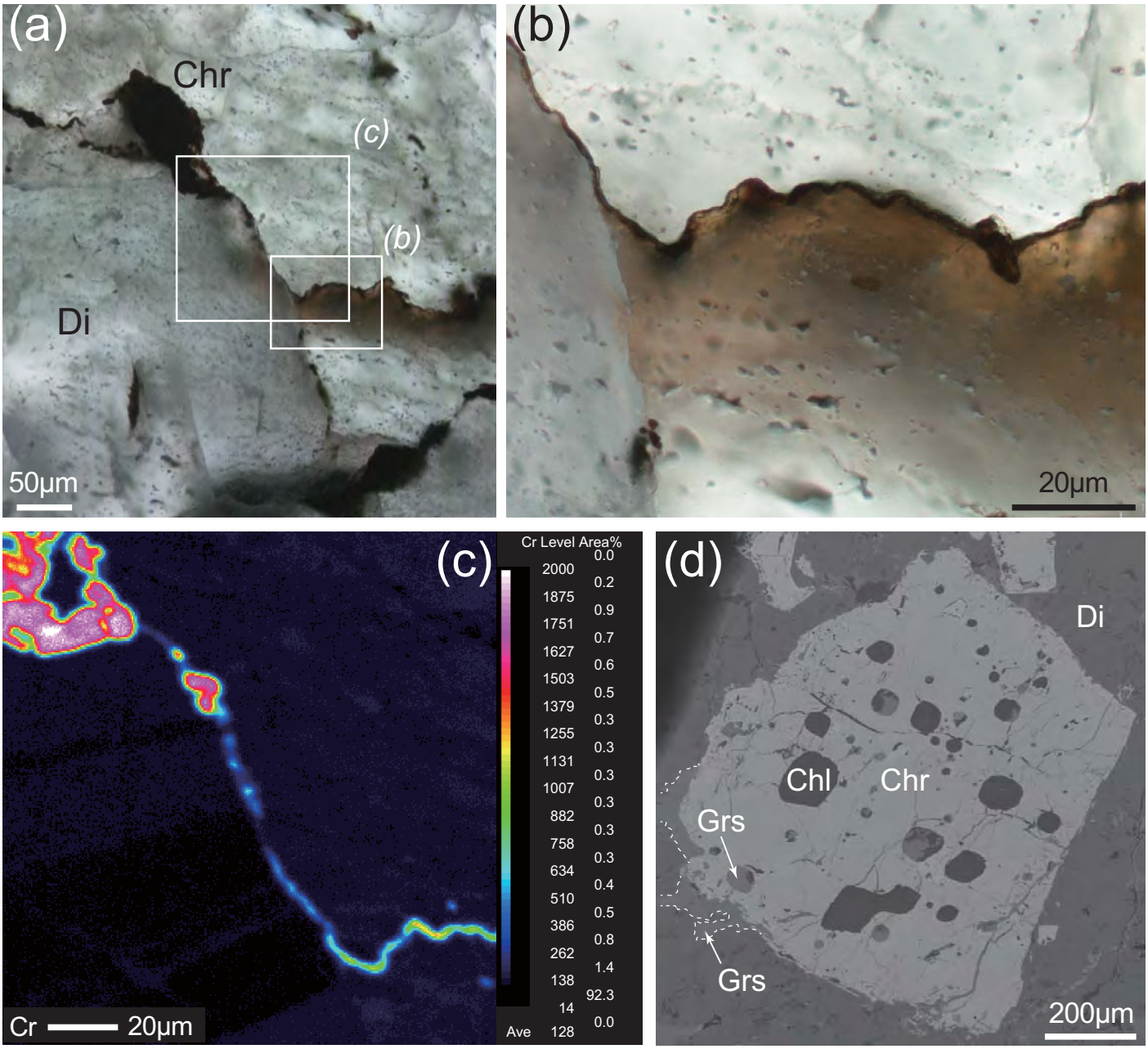

Arai & Akizawa Figure 3

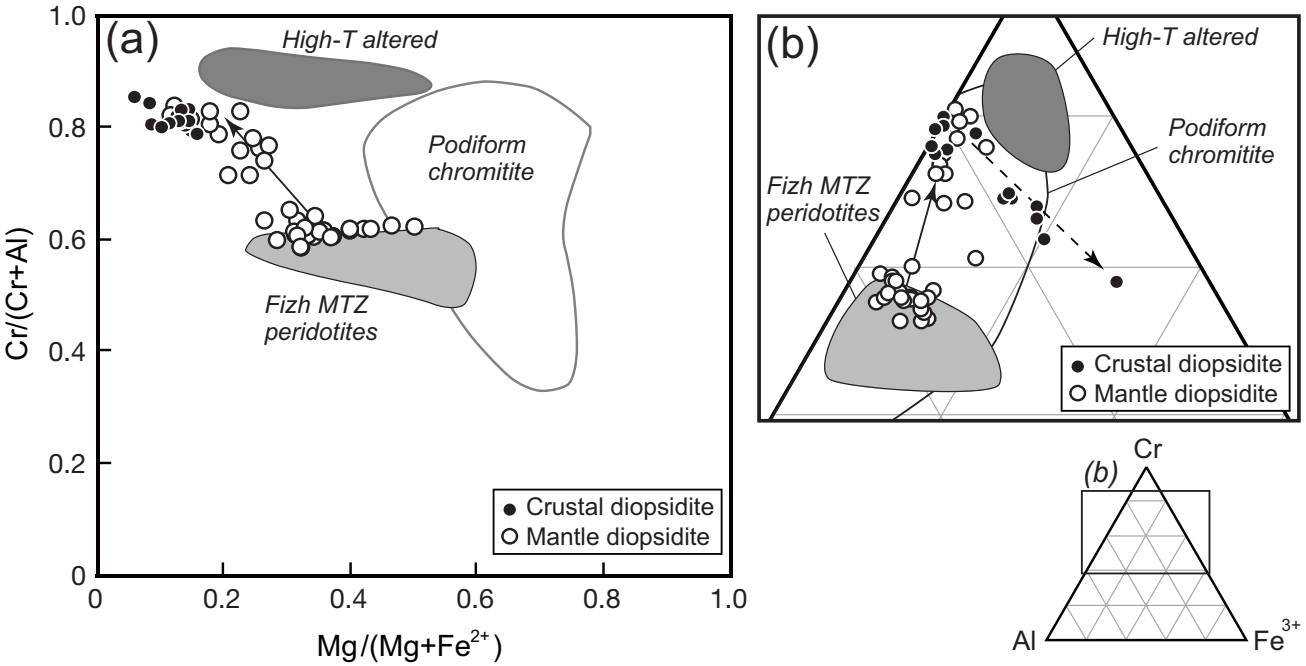

Figure 4 Arai and Akizawa

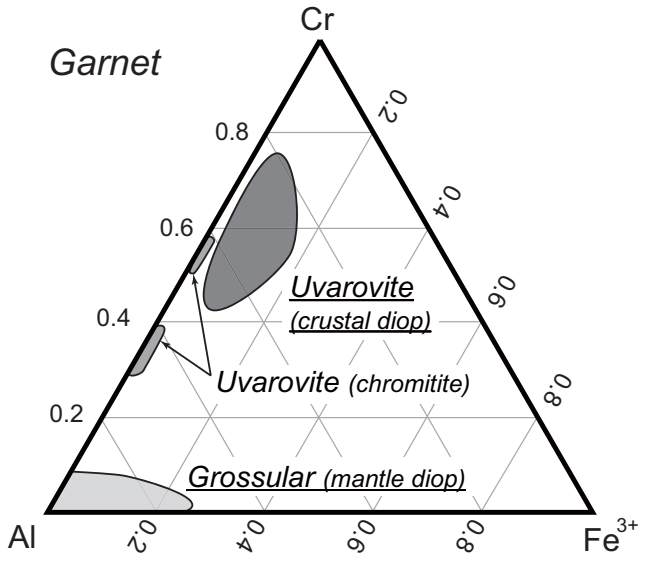

Figure 5 Arai and Akizawa